RESEARCH ARTICLE

Effect of lentiviral vector-mediated overexpression of hypoxia-inducible factor 1 alpha delivered by pluronic F-127 hydrogel on brachial plexus avulsion in rats

Tao Wang[1, 2, #], **Li-Ni Zeng**[1, #], **Zhe Zhu**[3, #], **Yu-Hui Wang**[1, 2], **Lu Ding**[4], **Wei-Bin Luo**[1, 2], **Xiao-Min Zhang**[1], **Zhi-Wei He**[1, *], **Hong-Fu Wu**[1, *]

1 Institute of Stem Cells and Regenerative Medicine, Department of Physiology, Guangdong Medical University, Dongguan, Guangdong Province, China

2 Department of Surgery, the Third Hospital of Guangdong Medical University (Longjiang Hospital of Shunde District), Foshan, Guangdong Province, China

3 Hand & Foot Surgery and Reparative & Reconstruction Surgery Center, the Second Hospital of Jilin University, Changchun, Jilin Province, China

4 Department of Scientific Research Center, the Seventh Affiliated Hospital, Sun Yat-Sen University, Shenzhen, Guangdong Province, China

Funding: *This work was financially supported by the National Natural Science Foundation of China, No. 81371366 (to HFW); the Natural Science Foundation of Guangdong Province of China, No. 2015A030313515 (to HFW); the Dongguan International Science and Technology Cooperation Project, No. 2013508152010 (to HFW); the Key Project of Social Development of Dongguan of China, No. 20185071521640 (to HFW).*

Graphical Abstract

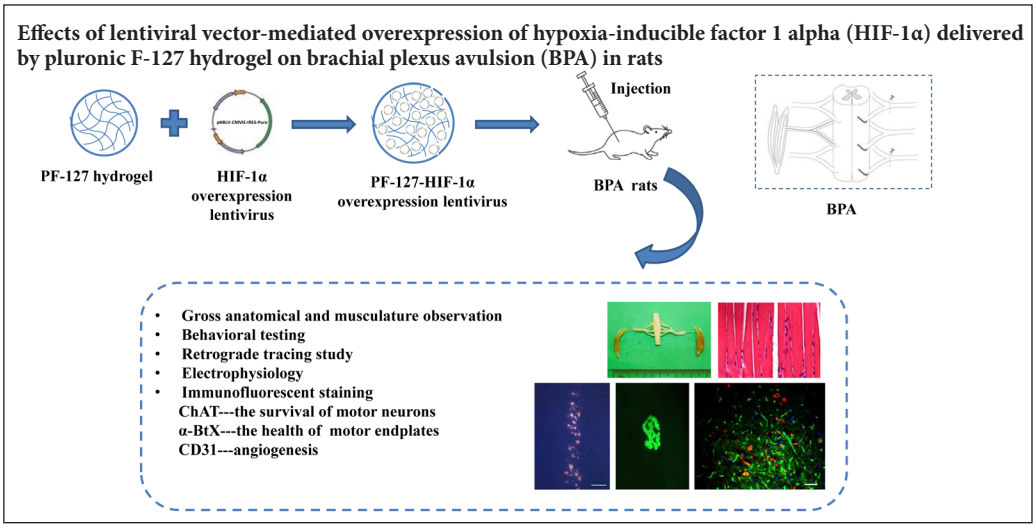

Correspondence to:
Zhi-Wei He, PhD, 467853605@qq.com;
Hong-Fu Wu, PhD, hongfuw@126.com.

#These authors contributed equally to this paper.

orcid:
0000-0002-3914-4752 (Zhi-Wei He)
0000-0002-1115-3681 (Hong-Fu Wu)

doi: *10.4103/1673-5374.250629*

Received: *October 11, 2018*
Accepted: *January 15, 2019*

Abstract

Brachial plexus avulsion often results in massive motor neuron death and severe functional deficits of target muscles. However, no satisfactory treatment is currently available. Hypoxia-inducible factor 1α is a critical molecule targeting several genes associated with ischemia-hypoxia damage and angiogenesis. In this study, a rat model of brachial plexus avulsion-reimplantation was established, in which C5–7 ventral nerve roots were avulsed and only the C6 root reimplanted. Different implants were immediately injected using a microsyringe into the avulsion-reimplantation site of the C6 root post-brachial plexus avulsion. Rats were randomly divided into five groups: phosphate-buffered saline, negative control of lentivirus, hypoxia-inducible factor 1α (hypoxia-inducible factor 1α overexpression lentivirus), gel (pluronic F-127 hydrogel), and gel + hypoxia-inducible factor 1α (pluronic F-127 hydrogel + hypoxia-inducible factor 1α overexpression lentivirus). The Terzis grooming test was performed to assess recovery of motor function. Scores were higher in the hypoxia-inducible factor 1α and gel + hypoxia-inducible factor 1α groups (in particular the gel + hypoxia-inducible factor 1α group) compared with the phosphate-buffered saline group. Electrophysiology, fluorogold retrograde tracing, and immunofluorescent staining were further performed to investigate neural pathway reconstruction and changes of neurons, motor endplates, and angiogenesis. Compared with the phosphate-buffered saline group, action potential latency of musculocutaneous nerves was markedly shortened in the hypoxia-inducible factor 1α and gel + hypoxia-inducible factor 1α groups. Meanwhile, the number of fluorogold-positive cells and ChAT-positive neurons, neovascular area (labeled by CD31 around av ulsed sites in ipsilateral spinal cord segments), and the number of motor endplates in biceps brachii (identified by α-bungarotoxin) were all visibly increased, as well as the morphology of motor endplate in biceps brachil was clear in the hypoxia-inducible factor 1α and gel + hypoxia-inducible factor 1α groups. Taken together, delivery of hypoxia-inducible factor 1α overexpression lentiviral vectors mediated by pluronic F-127 effectively promotes spinal root regeneration and functional recovery post-brachial plexus avulsion. All animal procedures were approved by the Institutional Animal Care and Use Committee of Guangdong Medical University, China.

Key Words: *nerve regeneration; peripheral nerve injury; brachial plexus avulsion; hypoxia; ischemia; hypoxia-inducible factor 1α overexpression; pluronic F-127; motor neurons; axonal regeneration; angiogenesis; neural regeneration*

Chinese Library Classification No. *R453; R364; R741*

Introduction

Brachial plexus avulsion is a severe injury mainly caused by traction of spinal cord roots due to physical damage such as injury from traffic accidents (Wang et al., 2015). It is often accompanied by massive motor neuron loss, which leads to severe functional deficits of the upper extremities (Chin et al., 2017). To date, surgery is the most frequently used treatment for brachial plexus avulsion, and several surgical methods have been attempted. Peripheral nerve transplantation and ventral root implantation are two common types of operation to restore the connection between motor neurons and their target muscles after brachial plexus avulsion (Bertelli and Mira, 1994; Gu et al., 2004). Direct reimplantation of the avulsed nerve root into the affected spinal cord can induce axonal regeneration and reinnervate muscle targets, which is helpful for recovery of hand movement function and has therefore been widely studied (Chai et al., 2000; Su et al., 2013). Nonetheless, reimplantation alone is not enough to achieve satisfactory results (Henderson et al., 1994). Adequate blood supply is an important factor for successful nerve grafting, and muscle reinnervation with vascularized nerve grafts is 20% faster than with nerve grafts only (Breidenbach and Terzis, 1984; Bertelli et al., 1996). Thus, assurance of an adequate blood supply (which protects ischemic cells from death) may be necessary for an ideal treatment outcome of brachial plexus avulsion (Cibert-Goton et al., 2015).

Hypoxia-inducible factor 1 (HIF-1) is a heterodimeric transcription factor that consists of an oxygen-regulated α-subunit and a constitutive β-subunit (Chai et al., 2014; Khan et al., 2017). HIF-1 is induced after hypoxia, ischemia, and inflammation, and plays an important role in several diseases such as Parkinson's disease, neonatal brain damage, acute cerebral ischemia, and ischemia necrosis of femoral head (Feng et al., 2014; Wang et al., 2014; Sun et al., 2017; Hu et al., 2018). HIF-1α is a member of the HIF family and has been intensively investigated for its special role in modulation of hypoxic-ischemic injury (Fan et al., 2009). Moreover, HIF-1α activation can trigger expression of vascular endothelial growth factor, which participates in angiogenesis (Kizaka-Kondoh et al., 2003; Gessi et al., 2013; Shan et al., 2013; Li et al., 2017). HIF-1α can also produce a strong protective effect on cortical neurons following ischemia-reperfusion-related injury *via* HIF-1α-independent mechanisms (Li et al., 2011). Thus, HIF-1α may have positive effects on angiogenesis, neuronal survival, and adaptation of ischemia-hypoxia, which suggests promising potential of HIF-1α application in brachial plexus avulsion therapy.

Furthermore, because of blood circulatory disorder triggered by brachial plexus avulsion, drug delivery *via* systemic circulation cannot easily reach the effective concentration. Directly injecting drugs, such as lithium and brain-derived neurotrophic factor, into damaged locations to repair brachial plexus avulsion injury has been reported (Chen et al., 2013; Fang et al., 2016). However, brachial plexus avulsion injury often results in irregular shape of the lesion cavity, as it may induce a high rate of drug loss and cause difficultly in localization to target cells or tissue. Thus, a delayed-release scaffold to release drugs to the injured site is important and valuable for brachial plexus avulsion treatment. Pluronic F-127 (PF-127) is a thermosensitive hydrogel that can change from a liquid to a gelatinous state within a suitable range of temperature. PF-127 has been approved by the Food and Drug Administration, and used widely in tissue engineering because of various favorable properties such as non-toxicity, biocompatibility, and biodegradability (Pandit and McGowan, 1998; Hao et al., 2014; Shen et al., 2015). We previously succeeded in grafting lentiviral vector into spinal cord injury animals *via* PF-127 encapsulation (Wu et al., 2013). Consequently, here we chose PF-127 as a carrier to deliver lentiviral vector-mediated HIF-1α overexpression at the injury site to increase viral transfection efficiency and determine whether co-grafting can facilitate recovery of brachial plexus avulsion injury. We hypothesized that this strategy may be of benefit to repair of similar nerve injuries.

Materials and Methods

Animals

Eighty female Sprague-Dawley rats aged 8–10 weeks and weighing 180–200 g were obtained from the Experimental Animal Center of Southern Medical University, China (license No. 44002100016020). All animal procedures were conducted in accordance with guidelines reviewed and approved by the Institutional Animal Care and Use Committee of Guangdong Medical University, China, and in accordance with the Guide for the Care and Use of Laboratory Animals as adopted and promulgated by the U.S. National Institutes of Health (Publication No. 85-23, revised 1996).

Lentiviral vector construction

The pHBLV-CMVIE-IRES-Puro lentiviral vector for HIF-1α overexpression was supplied by HANBIO Company (Shanghai, China). Final lentiviral vector titers contained 2×10^8 TU/mL.

Preparation of PF-127 hydrogel

PF-127 (Sigma-Aldrich, St. Louis, MO, USA) was prepared as a 25% (w/v) suspension in 0.1 M phosphate-buffered saline (PBS, pH 7.6). The mixture was shaken gently overnight at 4°C until complete dissolution and then filtered (0.22 μm aperture) and stored at 4°C until further use.

Before injecting into the brachial plexus avulsion model, lentiviral vectors (2×10^8 TU/mL) were mixed with 25% PF-127 on ice to obtain a final lentiviral vector concentration of 2×10^7 TU/mL. All procedures were conducted under sterile conditions.

Brachial plexus avulsion-reimplantation model

All rats were intraperitoneally anaesthetized with 1% pentobarbital sodium (40 mg/kg). The skin and muscles were incised along the midline of the animal body to expose spinal segments from the 4th cervical (C4) to 2nd thoracic (T2) lamina. Unilateral dorsal laminectomy was subsequently performed on the right C5 to C7 laminae to expose the dorsal roots. Using a stereomicroscope, the right C5–7 dorsal roots were removed using microscissors, and the corresponding

ventral roots avulsed using a slender glass hook. Part of the C5 and C7 spinal nerves were cut, leaving a gap of approximately 5 mm between the nerve roots and spinal cord. Meanwhile the C6 ventral root was replanted to the avulsed site for regeneration (**Figure 1A**). Thus, the brachial plexus avulsion-reimplantation model was established. The Terzis grooming test was performed one day after surgery. Rats scoring 0 indicated successful modeling. During surgery, care was taken to avoid additional spinal cord injury.

Group assignment and processing

Brachial plexus avulsion rats were randomly divided into five groups (n = 16): PBS, negative control of lentivirus (NV), gel, HIF-1α, and gel + HIF-1α. In each group after model establishment, implants were immediately transplanted into the avulsion site of the C6 ventral root with a microinjector: specifically 10 μL PBS, 1 μL negative control lentivirus suspension + 9 μL PBS, 10 μL gel, 1 μL HIF-1α overexpression lentivirus suspension + 9 μL PBS, and 1 μL HIF-1α overexpression lentivirus + 9 μL gel. The implant was slowly injected into the gap between the C6 ventral root and avulsed site using a sterile glass microsyringe. After transplantation, rats were kept in specific-pathogen-free conditions and treated by penicillin streptomycin injection (10,000 U/mL; Thermo Fisher Scientific, Waltham, MA, USA) during the first 3 days post-operation.

Quantitative real-time polymerase chain reaction (qRT-PCR)

To detect HIF-1α mRNA expression, qRT-PCR analysis was performed 1 week after surgery. According to the manufacturer's instructions, total RNA was extracted from C5–7 spinal segments using Trizol (Thermo Fisher Scientific). cDNA was reverse transcribed using the PrimeScript RT reagent Kit (TaKaRa, Tokyo, Japan). qRT-PCR was performed using SYBR Premix Ex Taq (TaKaRa). Relative mRNA expression from each sample was normalized to β-actin levels. Gene expression analysis was performed by the $2^{-\Delta\Delta Ct}$ method (EL-Badawy et al., 2017). Primer sequences of HIF-1α and β-actin are listed in **Table 1**.

Western blot assay

Western blot assay was performed 1 week after surgery. Harvested tissue from C5–7 spinal segments was homogenized in radioimmunoprecipitation assay lysis buffer (Millipore, Bedford, MA, USA) supplemented with phenylmethyl sulfonyl fluoride (Millipore) and mammalian protease inhibitor mixture (Biocolor Bioscience, Shanghai, China). Protein lysates were immunoblotted in accordance with a standard western blotting protocol. Briefly, samples were subjected to sodium dodecyl sulphate-polyacrylamide gel electrophoresis for separation, transferred to polyvinylidene fluoride membrane (0.2 μm; Millipore), and blocked with 5% non-fat milk for 2 hours at room temperature. Membranes were subsequently incubated overnight with the following primary antibodies at 4°C: HIF-1α (polyclonal antibody, rabbit anti-rat, 1:1000; Cell Signaling Technology, Danvers, MA, USA) and glyceraldehyde 3-phosphate dehydrogenase (GAPDH) (polyclonal antibody, mouse anti-rat, 1:1000; Thermo Fisher Scientific). After washing three times in Tris-buffered saline with Tween-20, primary antibodies were detected with secondary antibodies for 2 hours at room temperature: horseradish peroxidase goat anti-mouse/rabbit IgG (1:5000; ABclonal, Cambridge, MA, USA). Signals were digitally scanned and then quantified by ImageJ 1.6.0 software (National Institutes of Health, Bethesda, MD, USA). The results were represented as gray values. GAPDH was used as the internal control.

Table 1 Primer sequences

Gene	Sequence (5′–3′)	Product size (bp)
HIF-1α	F: 5′-gga tct att tcc ggt gaa ttc gcc acc ATG GAG GGC GCC GGC G-3′	2472
	R: 5′-tag aac tag tct cga gga att cTC AGT TAA CTT GAT CCA AA-3′	
β-Actin	F: 5′-CAC GAT GGA GGG GCC GGA-3′	93
	R: 5′-TAA AGA CCT CTA TGC CAA-3′	

In HIF-1α primer sequences, lowercase letters represent lentiviral vector gene sequence and uppercase letters represent HIF-1α gene sequence. HIF-1α: Hypoxia-inducible factor 1α; F: forward primer; R: reverse primer.

Gross specimen

At the end of 6 weeks, four rats from each group were perfused and C5–7 cervical vertebra segments extracted along with both sides of forelimbs. Dorsal laminectomy was performed to expose the dorsal spinal cord and peripheral nerve roots. Bilateral biceps and coterminous musculocutaneous nerves were carefully separated. Finally, the cervical cord, bilateral brachial plexus, both sides of musculocutaneous nerves, and biceps were integrally separated. The gross specimen was fixed in 4% paraformaldehyde at 4°C for further observation.

Dry weight ratio of biceps brachii

Biceps tissue was collected at the 6-week endpoint after surgery and the dry weight ratio calculated (four rats per group). Affected and healthy biceps from brachial plexus avulsion rats in each group were heated in a 90°C oven for 48 hours until the difference between two consecutive weighing's was < 0.2 mg. The dry weight ratio of ipsilateral to contralateral biceps was calculated.

Hematoxylin and eosin staining

Paraffin cross sections of biceps were collected from two rats in each group at the 6-week endpoint. Sections were dewaxed twice in xylene (5 minutes each). After rehydrating in a series of graded alcohol, sections were washed in distilled water for 2 minutes. Bicep sections were stained with hematoxylin solution for 10 minutes, differentiated in 1% acid alcohol for 30 seconds, soaked in running water, and then counterstained with eosin solution for 30–60 seconds. After washing in running water for 5 minutes, tissue samples were again dehydrated in a series of graded alcohol (5 minutes each), cleared in xylene (I, II; 5 minutes each), and mounted with neutral balsam. For each bicep, more than six fields were randomly photographed with a light microscope (20×,

ECLIPSE TS100; Nikon, Tokyo, Japan). Muscle fiber diameter was quantified using ImageJ 1.6.0 software. The extent of fibrosis was determined by the ratio of fibroblast nuclei number in ipsilateral to contralateral biceps.

Behavioral testing

The Terzis grooming test was performed to evaluate motor function of the upper limbs (Bertelli and Mira, 1993). Each rat was placed in a spacious and quiet environment. Bacteria-free water was gradually sprayed on the head and neck of animals with a 60-mL syringe to elicit bilateral grooming behavior of the upper limbs. Movement of the right upper limb was assessed by the following rating criteria: grade 0, no response; grade 1, elbow flexion but unable to touch nose; grade 2, elbow flexion and able to touch nose; grade 3, elbow flexion and able to reach the site below the eyes; grade 4, elbow flexion and able to reach the eyes; and grade 5, elbow flexion and able to reach the ears or back of the ears (Bertelli and Mira, 1993). Two days before operation, bilateral grooming behavior was successfully elicited in all animals; each rat scored 5. At 24 hours post-surgery, rats were reevaluated. Successful surgery was confirmed if rats scored 0. The Terzis grooming test was evaluated and recorded weekly from the second week post-surgery to the endpoint. Observations were made by two observers who were blinded to the subgroups.

Electrophysiology

Two days before perfusion, four rats from each group were administered general anesthetic. The skin and muscle were opened to expose the right biceps brachii and homolateral musculocutaneous nerve. The musculocutaneous nerve was partially hooked onto a pair of stimulation electrodes, while another pair of recoding needle electrodes were inserted into the biceps at a depth of 1–2 mm with a distance of 3–9 mm. Electrical stimuli ranging from 0.8–1.2 V were applied, and the motor evoked potential recorded from the biceps using needle electrodes. In one biceps, electrical activity was performed at three different motor unit locations. Stimulation was delivered for each trial by an electrical stimulator from MedLab Biological Signal Collection System (Meiyi Technology Ltd., Nanjing, China).

Fluorogold retrograde tracing

Fluorogold retrograde labeling of spinal motor neurons was performed in accordance with a previous study (Gu et al., 2004). Briefly, four rats from each group were re-anesthetized and the right musculocutaneous nerve re-exposed under stereoscopic microscopy. Four rats from each group were injected with fluorogold at the 6-week endpoint and two days before perfusion. A total of 2 μL fluorogold (Sigma-Aldrich) was slowly injected into the musculocutaneous nerve using a micropump at 4.0 ± 0.5 mm distal to the avulsed site of the lateral cord. The muscle and skin were routinely sutured. At 2 days post-injection, rats were perfused and C5–7 spinal segments separated. Tissue was fixed using 4% paraformaldehyde (Solarbio, Beijing, China) for 6–8 hours and then dehydrated in 30% sucrose for 2 days. Spinal segments were sliced into 20 μm frozen sections. Fluorogold-labeled neurons in the ipsilateral C5–7 ventral horn were calculated under fluorescence microscopy (Carl–Zeiss Axioplan 2 imaging E, Baden–Wurttemberg, Germany).

Immunofluorescence

The immunofluorescence procedure was similar to the method performed in our previous study (three rats per group) (Diniz et al., 2015). The primary antibodies used were: rabbit polyclonal anti-choline acetyltransferase (ChAT) (motoneuron marker; 1:200; Millipore), rabbit polyclonal anti-α-bungarotoxin (α-BtX) (motor endplate-targeting marker; 1:400; Thermo Fisher Scientific), mouse polyclonal anti-CD31 (angiogenesis marker; 1:200; Millipore), and rabbit polyclonal anti-NeuN (neuronal marker; 1:200; Millipore). The secondary antibody used was mouse anti-rat conjugated to Alexa Fluor 568 or goat anti-rat conjugated to Alexa Fluor 488 (1:400, Thermo Fisher Scientific). Briefly, sections were permeabilized in 0.3% Triton X-100 for 15 minutes and then blocked in 10% natural goat serum (diluted in PBS) for 30 minutes. Afterwards, sections were incubated with primary antibodies overnight at 4°C and then washed three times in PBS. Next, tissue was incubated with secondary antibody in the dark for one hour at 37°C. After repeated washes, samples were counterstained with 4′,6-diamidino-2-phenylindole (DAPI) (1:5000, Cell Signaling Technology) for 10 minutes. Fluorescence Mounting Medium (Dako, Copenhagen, Denmark) was used to mount tissue onto coverslips. Finally, samples were examined under a fluorescence microscope (Carl-Zeiss Axioplan 2 imaging E).

Calculation of motor endplates and neurovascular area

Fourteen μm-thick longitudinal sections of biceps or spinal cord were collected and stained with α-BtX antibody (1:500; Alexa Fluor 488 conjugated; Thermo Fisher Scientific) and CD31 (1:1000; Alexa Fluor 488 conjugated; Wako, Osaka, Japan), respectively. Under fluorescence microscopy, motor endplates in biceps were captured and counted. Next, 100–200 motor endplates from each bicep were randomly chosen to measure motor endplate area using ImageJ 1.6.0 software. Average motor endplate area was calculated in each group. To calculate neurovascular area in spinal cord sections, angiogenesis within approximately 5 mm from the avulsed site was observed and randomly photographed using a fluorescence microscope. The area of new blood vessels was also measured using ImageJ.

Statistical analysis

Data are presented as the mean ± SD. All statistical data were analyzed using SPSS 20.0 statistical software (IBM, Armonk, NY, USA). One-way analysis of variance followed by the least significant difference or Bonferroni *post hoc* tests was selected depending on the number of groups. All tests were two-tailed and values of $P < 0.05$ were considered statistically significant.

Results

Lentiviral vector effectively upregulates HIF-1α expression in the spinal cord

To investigate the efficiency of HIF-1α lentivirus overexpression, rats were subjected to brachial plexus avulsion (**Figure 1Aa**) and HIF-1α lentivirus overexpression. Additionally, a compound of gel + HIF-1α was injected into the avulsed site post-ventral root reimplantation (**Figure 1Ab**). C5–7 spinal tissue was extracted from rats in the HIF-1α and gel + HIF-1α groups, and HIF-1α mRNA and protein levels detected at 7 days post-brachial plexus avulsion. qRT-PCR (**Figure 1B**) showed significantly increased HIF-1α mRNA levels after lowering HIF-1α lentivirus overexpression with or without hydrogel. Specifically, relative amounts of HIF-1α mRNA were higher in the HIF-1α and gel + HIF-1α groups compared with the PBS group ($P < 0.001$). Western blot assay (**Figure 1C**) showed similar trends ($P < 0.001$). Together, this demonstrates that delivery of HIF-1α-overexpressing lentiviral vector *in vivo* effectively upregulates HIF-1α expression post-brachial plexus avulsion.

Gross anatomical and musculature observations

Brachial plexus avulsion rats were perfused at a 6-week endpoint, and the gross anatomy carefully dissected. C5 and C7 were completely avulsed, while C6 was closely attached to the ventrolateral surface of the spinal cord, demonstrating successful reimplantation of C6. In all groups, ipsilateral biceps were atrophied compared with contralateral ones (**Figure 2A**), which might result from denervation and deficiency of tropism derived from motor neuron axons. Simultaneously, the dry weight ratio of bilateral biceps was significantly higher in the HIF-1α ($P < 0.01$) and gel + HIF-1α groups (64.7% and 66.7%, respectively; $P < 0.01$; **Figure 2B**). There were no obvious differences between the PBS (43.4%) and NV (43.60%) groups.

As previously reported, motor neurons are unable to provide trophic support for muscle fibers to maintain the normal morphology and function of innervated organs after brachial plexus avulsion (Ali et al., 2016). Thus, muscle fiber atrophy often leads to degradation and loss of motor function. Accordingly, we next observed structural features of bicep cross sections by hematoxylin-eosin staining. As shown in **Figure 2C**, muscle fibers exhibited much smaller diameters in the PBS and NV groups. In contrast, muscle fibers were larger with clear myocyte nuclei in the gel, HIF-1α, and gel + HIF-1α groups, particularly in the HIF-1α and gel + HIF-1α groups ($P < 0.01$). In the HIF-1α and gel + HIF-1α groups, 53% of muscle fibers had diameters larger than 30 μm. Only 20% of muscle fibers in the PBS and NV groups were of comparable size (**Figure 2D**). The extent of muscle fibrosis was evaluated from the ratio of fibroblast nuclei in ipsilateral to contralateral biceps. Accordingly, muscle fibrosis was significantly reduced in the HIF-1α ($P < 0.01$) and gel + HIF-1α groups ($P < 0.001$), particularly in the gel + HIF-1α group (**Figure 2E**).

Co-transplantation promotes recovery of motor function post-brachial plexus avulsion

Movement of the right forelimb was assessed by the Terzis grooming test. As shown in **Figure 3A**, Terzis grooming test scores were higher in the HIF-1α ($P < 0.05$) and gel + HIF-1α ($P < 0.001$) groups compared with the PBS group from the second week to endpoint post-brachial plexus avulsion (**Figure 3A**). At 6 weeks post-surgery, 66.7% and 91.7% of rats scored ≥ 4 in the HIF-1α and gel + HIF-1α groups, respectively. Only 41.7% of rats obtained this level in the PBS group (**Figure 3B**). These findings show that motor function recovery was markedly better in the gel + HIF-1α group than HIF-1α group.

To further determine whether functional recovery was associated with electrophysiological restoration of forelimb function, electrophysiology testing was performed at 6 weeks post-surgery. Electrophysiology testing is an obligatory clinical examination that provides reliable evidence of denervation and fasciculation in peripheral neuropathy (Mills, 2005). Latency of motor evoked potentials was shorter in the HIF-1α (1.15 ± 0.05 ms) and gel + HIF-1α (1.13 ± 0.03 ms) groups than in the other groups. Mean latency detected in the PBS group was 1.27 ± 0.03 ms. The amplitude of motor evoked potentials was higher in the HIF-1α and gel + HIF-1α groups than in the other treatment groups (**Figure 3C** and **D**). Moreover, latency was slightly shorter in the gel group than PBS and NV groups ($P < 0.05$). This suggests that gel may be a significant factor in the bridging role, and

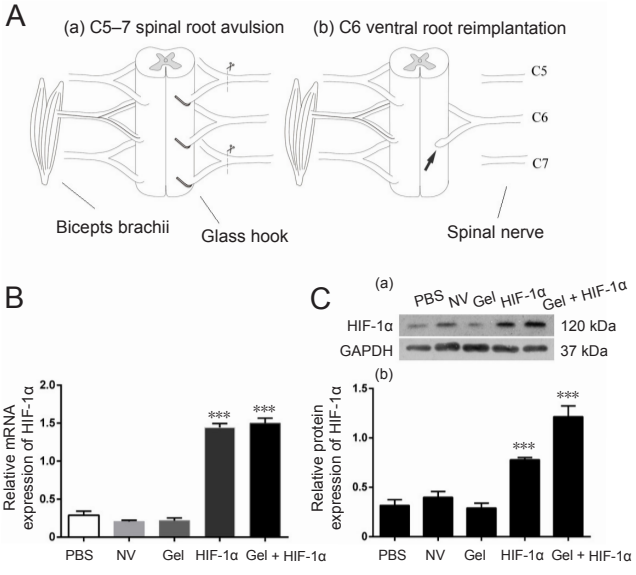

Figure 1 Brachial plexus avulsion-reimplantation model and efficiency of HIF-1α overexpression.

(A) Unilateral avulsion of C5–7 nerve roots (a) and reimplantation of C6 on the ventral surface of the corresponding spinal segment (b). The black arrow indicates the lentivirus injection site. (B) mRNA expression of HIF-1α in C5–7 spinal cord segments measured by qRT-PCR were significantly increased in rats treated with both HIF-1α and gel + HIF-1α. mRNA expression was determined by the ΔΔCt method. β-Actin was used as the internal control. (C) Western blot assay (a) and quantification of HIF-1α protein (b) demonstrated marked upregulation of HIF-1α in the HIF-1α and gel + HIF-1α groups. GAPDH was used as the internal control. Data are presented as the mean ± SD ($n = 2$; one-way analysis of variance followed by the least significant difference *post hoc* test). ***$P < 0.001$, *vs.* PBS group. GAPDH: Glyceraldehyde phosphate dehydrogenase; PBS: phosphate buffered saline; NV: negative control of lentivirus; Gel: PF-127 hydrogel; HIF-1α: hypoxia-inducible factor 1α overexpression lentivirus; Gel + HIF-1α: PF-127 hydrogel combined with hypoxia-inducible factor 1α overexpression lentivirus.

that porous spatial structure benefits nerve regeneration. Consequently, gel transplantation alone may also enhance reconstruction of neural pathways to a certain extent.

Co-implantation facilitates axonal regeneration post-brachial plexus avulsion

Axonal regeneration of surviving motor neurons was next investigated using a retrograde tracing study. Ventral horn motor neurons were labeled by retrograde transport of fluorogold through regenerating axons (**Figure 4A**). In the PBS group, a small percentage of neurons were fluorogold-positive, while approximately 1.5-times fluorogold-labeled neurons were observed in the gel + HIF-1α group (**Figure 4B**; $P < 0.001$). Although more fluorogold-positive motor neurons were detected in rats treated with HIF-1α and gel + HIF-1α, the number of fluorogold-positive motor neurons was highest in the gel + HIF-1α group compared with other groups. These results suggest that the combined strategy efficiently promotes axonal regeneration of avulsed motor neurons and facilitates re-entry of regenerating axons into the peripheral nervous system.

Co-transplantation enhances survival of injured motor neurons post-brachial plexus avulsion

Avulsion injury usually induces severe motor neuron degeneration and death, which has a profound effect on subsequent nerve regeneration and tissue repair. To investigate the effect of co-transplantation on motor neuron survival after ventral root reimplantation, surviving motor neurons in avulsed C5–7 spinal cord segments were examined by the specific marker, ChAT (**Figure 4C**). Overall, there were 80% ChAT-positive motor neurons in the gel + HIF-1α group, with only approximately 65% in the PBS or NV groups ($P < 0.01$; **Figure 4D**). Additionally, a significant increase in survival rate of motor neurons was also obtained by HIF-1α lentivirus overexpression. Thus, these results show that HIF-1α lentivirus overexpression with or without gel effectively enhances the survival rate of motor neurons.

Co-implantation leads to healthy endplates post-brachial plexus avulsion

Motor endplates are considered to be postsynaptic folds of neuromuscular junctions, in which a high density of acetylcholine receptors (AChRs) are located and function to regulate contractile activity of skeletal muscle. α-BtX can specifically bind AChRs, and is used to stain muscle sections to assess the size and morphology changes of motor endplates. In rats with reimplantation alone, motor endplates tended to be faintly stained with an ambiguous appearance, suggesting obvious loss of AChRs as a consequence of weak reinnervation. In contrast, motor endplates in the gel + HIF-1α group were larger in size (**Figure 5A**). Regarding the area distribution of motor endplates, severe loss of AChRs was observed, with an average area of approximately 370 μm^2 in the PBS and NV groups. As shown in **Figure 5B**, motor endplate area was larger in the HIF-1α group ($P < 0.05$) and gel + HIF-1α group ($P < 0.001$), particularly the gel + HIF-1α group (458.4 ± 272 μm^2). These data indicate that a compound of gel + HIF-1α may exert a protective effect on neuromuscular junctions.

Co-transplantation facilitates neovascularization post-brachial plexus avulsion

Spinal root injury produces loss of vascular integrity, which contributes to enhancement of the secondary injury response that determines the extent of functional recovery (Benton et al., 2008; Cibert-Goton et al., 2015). Consequently, early revascularization is of great importance for nerve regeneration and tissue repair. To investigate formation of new blood vessels, we performed immunofluorescence using CD31, a surface marker of neovascular endothelial cells, and counterstained with NeuN, a specific marker of neurons. In the PBS and NV groups, there were few new vessels around neurons. Meanwhile, the number of new vessels was increased in the HIF-1α and gel + HIF-1α groups than the PBS and NV groups (**Figure 6A**). Notably, co-transplantation of HIF-1α ($P < 0.01$) and gel ($P < 0.05$) induced a significant increase of angiogenesis around neurons. Indeed, the average distribution area of nerves and blood vessels was nearly three-times more in the gel + HIF-1α group ($P < 0.001$) compared with the PBS and NV groups (**Figure 6B**). Thus, these immunofluorescence results show that gel and HIF-1α compound may promote angiogenesis, which is beneficial to neuronal survival.

Discussion

Brachial plexus avulsion injury is a lesion at the interface of the peripheral and central nervous systems, which triggers a hypoxic-ischemic inhibitory microenvironment and induces extensive degeneration of spinal motor neurons (Oliveira and Langone, 2000). Ventral root avulsion results in permanent loss of motor function in patients, thereby reducing their life quality. Although nerve transfer has been used clinically for many years, functional recovery after surgery is unsatisfactory (Romeo-Guitart et al., 2017). Nerve root reimplantation is an easy-to-operate and minimal deficit surgery that can induce axonal regeneration of injured motor neurons to reinnervate muscle targets and lead to recovery of motor function (Su et al., 2013). Li et al. (2015) demonstrated that after ventral root avulsion and immediate reimplantation, modulation of protein tyrosine phosphatase-σ (which is a neuronal receptor of chondroitin sulfate proteoglycans) by systemic delivery of intracellular sigma peptide, markedly enhanced regeneration (Li et al., 2015). In this study, to establish a brachial plexus avulsion model, we also avulsed C5–7 ventral nerve roots and then reimplanted C6 only (Li et al., 2015). Gross analysis showed that muscles on the affected side were visibly atrophic. Moreover, dry weight ratio of the affected to healthy side was markedly greater in the HIF-1α and gel + HIF-1α groups (and especially the gel + HIF-1α group) than the PBS and NV groups. These results suggest that co-transplantation of HIF-1α overexpression lentivirus plus gel effectively contributes to muscle morphology. Muscle fiber diameter is an important indicator of muscle reinnervation (Vleggeert-Lankamp, 2007). Hematoxylin-eosin staining of muscle

fibers has confirmed the above conclusion. A previous study reported that hypoxia can influence muscle fiber atrophy, while HIF-1α activation can improve adaptation of skeletal muscle to hypoxia (Favier et al., 2015). Here, we delivered HIF-1α lentivirus with PF-127 hydrogel to the lesion site, and induced HIF-1α overexpression, which may be beneficial for improving skeletal muscle adaptation to hypoxia.

The Terzis grooming test is often used to assess behavioral changes of brachial plexus avulsion rats (Hao et al., 2018). Compared with other groups, Terzis grooming test score was highest in the gel + HIF-1α group from the second week to endpoint after brachial plexus avulsion. This shows that co-transplantation of gel and HIF-1α promotes recovery of motor function after brachial plexus avulsion. Furthermore, motor evoked potential latency of musculocutaneous nerve was examined to assess restoration of the nerve-muscle electrical pathway. Latency represents the time from nerve stimulation to muscle contraction: shorter latencies indicate better nerve conduction capacity. Electrophysiological results showed the shortest motor evoked potential latency in the gel + HIF-1α group. Integrity of the motor unit (which consists of motor neurons, nerve fibers, and motor endplates) is important for nerve conduction. In this study, we examined the morphology of motor endplates by α-BtX staining. We found larger average motor endplate area mainly in the gel + HIF-1α group. This may indicate that regenerating motor axons in this group can reach the innervated target muscle more efficiently and facilitate recovery of motor function (Cullheim et al., 1989). Taken together, co-transplantation of gel and HIF-1α contributes to reconnection of neural pathways and facilitates recovery of upper limb motor function after brachial plexus avulsion injury.

Survival of affected motor neurons is ultimately important for axonal regeneration (Hallin et al., 1999; Li and Wu, 2017). Neurotrophic factors such as glial cell line-derived neurotrophic factor and brain-derived neurotrophic factor are beneficial to motor neuron survival, but high levels of neurotrophic factors prevent directional growth of axons of surviving motor neurons into implanted root (Blits et al., 2004). In this study, we used the specific marker, ChAT, to detect motor neurons in each group, providing further evidence for the protective role of gel + HIF-1α compound in neurons. A recent report showed that HIF-1α represents a critical transcriptional regulator in regenerating neurons and stimulating axonal regeneration under hypoxic conditions (Cho et al., 2015). Consequently, using HIF-1α overexpression lentivirus to protect surviving neurons may be beneficial. Appropriately, retrograde tracing confirmed that the number of fluorogold-positive cells was increased in the HIF-1α and gel + HIF-1α groups compared with the PBS, NV, gel, HIF-1α, and gel + HIF-1α groups. Thus, HIF-1α with or without gel treatment can increase survival of spinal motor neurons and may benefit reconstruction of neural pathways after brachial plexus avulsion. It has been widely demonstrated that HIF-1α is an important mediator of the hypoxic response and upregulates angiogenic factors, such as vascular endothelial growth factor (Sato et al., 2012). To verify the effect of gel and HIF-1α on angiogenesis, we investigated vascularization at the avulsed site by double immunofluorescence staining with a vascular endothelium specific antibody, CD31, and a neuronal marker, NeuN. Abundant neovascularization around neurons was observed in the gel + HIF-1α group compared with the PBS group. Because brachial plexus avulsion is a type of "longitudinal spinal cord" injury, trauma to the spinal cord results in disruption of the local blood vessel network and initiates a multifaceted pathophysiological response to injury, thereby causing endothelial cell death. Loss of microcirculation and impediment of the tissue repair process are due to deficiency of an adequate blood supply (Benton et al., 2008). Meanwhile, HIF-1α functions as an intrinsic modulator of vascular remodeling-related gene expression and plays a key role in neovascularization (Shan et al., 2013; Imanishi et al., 2014). We inferred that neovascularization may be due to HIF-1α overexpression at the lesion site because it can improve revascularization and supply blood and nutrients to the avulsion–reimplantation position of nerve roots and benefit neuronal survival. In this study, a certain degree of angiogenesis was observed in the gel group, presumably because PF-127 hydrogel serves as a sustained-controlled vector, which may play a role in stabilizing the C6 reimplantation nerve root on the surface of the spinal cord, and extending the time for effective concentration of lentiviral vector-mediated HIF-1α overexpression at the nerve avulsion site. Additionally, a previous study provided evidence that PF-127 can enhance cell attachment, collagen formation, and angiogenesis to a certain extent (Bensaid et al., 2003).

In conclusion, transplantation of lentiviral vector-mediated HIF-1α overexpression combined with PF-127 hydrogel into brachial plexus avulsion rats can improve recovery of motor function, reconstruction of the neural pathway, and protection of motor neurons. HIF-1α may have a positive effect on angiogenesis, neuronal survival, and adaptation of the ischemia-hypoxia condition. Although our experimental results show promising potential of gel and HIF-1α application in brachial plexus avulsion therapy, the molecular mechanism of HIF-1α on regulating functional recovery after brachial plexus avulsion has not been fully investigated. Therefore, further research on the relationship between HIF-1α and brachial plexus avulsion is needed to find a better therapy for brachial plexus avulsion injury.

Author contributions: *Obtaining funding and study design: HFW and ZWH; data collection and analysis: TW and ZZ; experimental implementation: LNZ, ZZ, YHW, WBL, XMZ and LD; manuscript writing: LNZ. All authors approved the final version of the paper.*
Conflicts of interest: *The authors declare that there are no conflicts of interest associated with this manuscript.*
Financial support: *This work was financially supported by the National Natural Science Foundation of China, No. 81371366 (to HFW); the Natural Science Foundation of Guangdong Province of China, No. 2015A030313515 (to HFW); the Dongguan International Science and Technology Cooperation Project, No. 2013508152010 (to HFW); the Key Project of Social Development of Dongguan of China, No. 20185071521640 (to HFW). The funding sources had no role in study conception and design, data analysis or interpretation, paper writing or deciding to submit this paper for publication.*
Institutional review board statement: *The animal procedures were conducted in accordance with guidelines reviewed and approved by the Institu-*

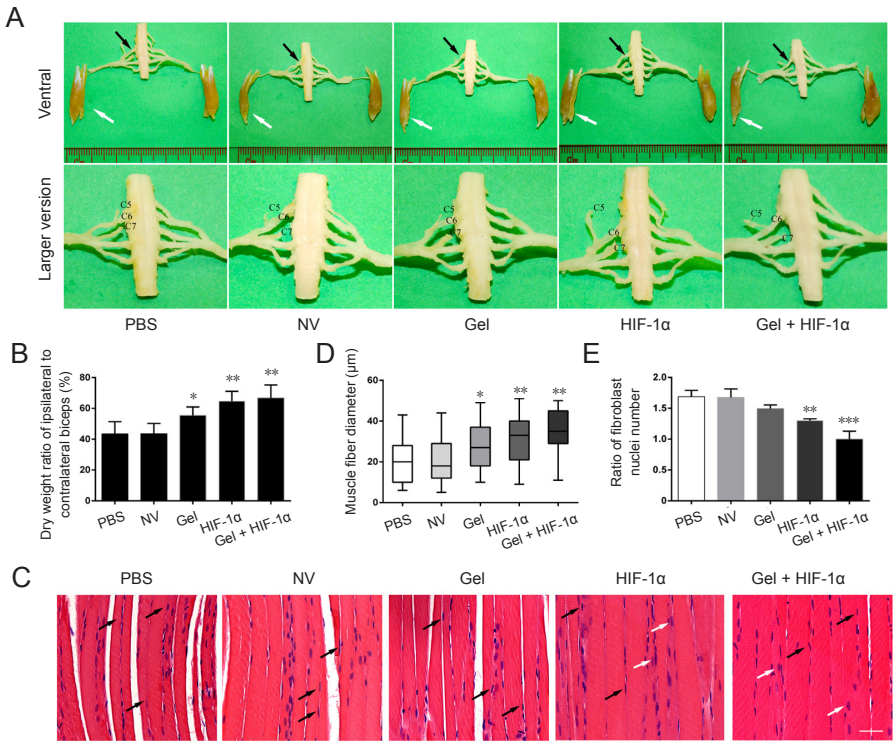

Figure 2 Gross anatomical and musculature observations at 6 weeks post-brachial plexus avulsion.
(A) Representative photographs of gross anatomical specimens of rats from different groups. Reimplanted C6 ventral roots (black arrows) closely attached to the ventrolateral surface of ipsilateral C6 spinal segments and regrew into spinal roots. In contrast, an obvious gap was observed between C5–7 spinal roots and the corresponding spinal segments. Atrophied biceps were observed on the ipsilateral side (white arrows). (B) Dry weight ratio of ipsilateral to contralateral biceps. (C) Representative photomicrographs of longitudinal bicep sections by hematoxylin-eosin staining: muscle fibers and fibroblast nuclei were observed by light microscopy. In PBS and NV groups, biceps with shrunken sarcoplasm and abundant fibroblast nuclei (black arrows) displayed severe muscle atrophy. Contrarily, HIF-1α and gel + HIF-1α treatment resulted in less extensive fibrosis, demonstrated by fewer fibroblast nuclei and an abundant clear myocyte nucleus (white arrows). Scale bar: 50 μm. (D) Quantitative analysis of muscle fiber diameter. (E) The extent of fibrosis was determined by the ratio of fibroblast nuclei number in ipsilateral to contralateral biceps. Data are presented as the mean ± SD (n = 2; one-way analysis of variance followed by the least significant difference [B, D] or Bonferroni [E] *post hoc* test). $*P < 0.05$, $**P < 0.01$, $***P < 0.001$, *vs.* PBS group. PBS: Phosphate buffered saline; NV: negative control of lentivirus; Gel: PF-127 hydrogel; HIF-1α: hypoxia-inducible factor 1α overexpression lentivirus; Gel + HIF-1α: PF-127 hydrogel combined with hypoxia-inducible factor 1α overexpression lentivirus.

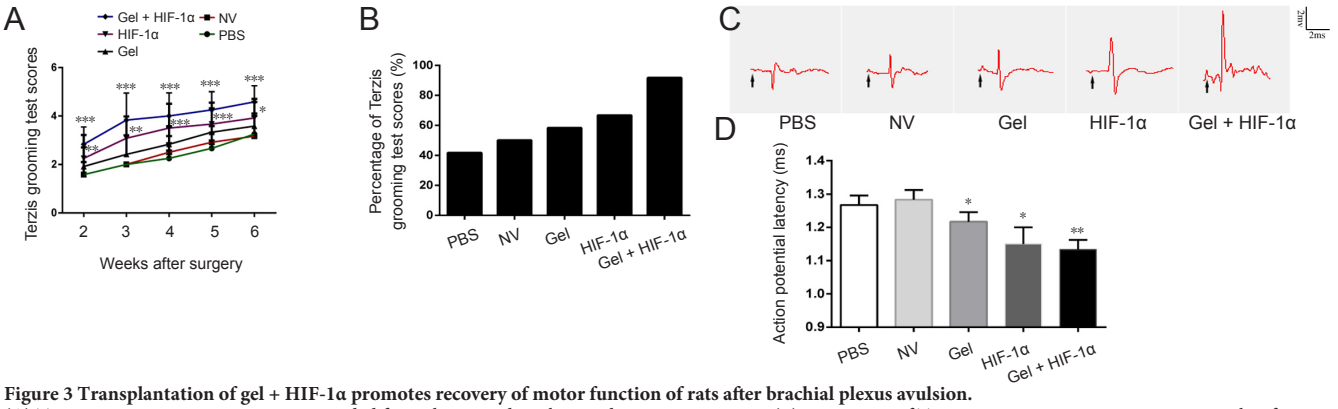

Figure 3 Transplantation of gel + HIF-1α promotes recovery of motor function of rats after brachial plexus avulsion.
(A) Terzis grooming test scores were recorded from the second week to endpoint post-surgery. (B) Percentage of Terzis grooming test scores ≥ 4 at 6 weeks after surgery among different groups. Significant functional improvement was achieved in the gel + HIF-1α group. (C) Electrophysiological responses of musculocutaneous nerve in each subgroup. Black arrows represent the stimulus mark. (D) Action potential latency of musculocutaneous nerve in each group at 6 weeks after surgery. Data are presented as the mean ± SD (n = 4; one-way analysis of variance followed by the least significant difference *post hoc* test). $*P < 0.05$, $**P < 0.01$, $***P < 0.001$, *vs.* PBS group. TGT: Terzis grooming test; PBS: phosphate buffered saline; NV: negative control of lentivirus; Gel: PF-127 hydrogel; HIF-1α: hypoxia-inducible factor 1α overexpression lentivirus; Gel + HIF-1α: PF-127 hydrogel combined with hypoxia-inducible factor 1α overexpression lentivirus.

tional Animal Care and Use Committee of Guangdong Medical University, China. All experimental procedures described here were in accordance with the National Institutes of Health (NIH) guidelines for the Care and Use of Laboratory Animals (NIH Publication No. 85-23, revised 1986).

Data sharing statement: *Datasets analyzed during the current study are available from the corresponding author on reasonable request.*

Plagiarism check: *Checked twice by iThenticate.*

Peer review: *Externally peer reviewed.*

Open peer reviewer: *Huiyin Tu, Zhengzhou University, China*

Additional file: *Open peer review report 1.*

References

Ali ZS, Johnson VE, Stewart W, Zager EL, Xiao R, Heuer GG, Weber MT, Mallela AN, Smith DH (2016) Neuropathological characteristics of brachial plexus avulsion injury with and without concomitant spinal cord injury. J Neuropathol Exp Neurol 75:69-85.

Bensaid W, Triffitt JT, Blanchat C, Oudina K, Sedel L, Petite H (2003) A biodegradable fibrin scaffold for mesenchymal stem cell transplantation. Biomaterials 24:2497-2502.

Benton RL, Maddie MA, Minnillo DR, Hagg T, Whittemore SR (2008) Griffonia simplicifolia isolectin B4 identifies a specific subpopulation of angiogenic blood vessels following contusive spinal cord injury in the adult mouse. J Comp Neurol 507:1031-1052.

Bertelli JA, Mira JC (1993) Behavioral evaluating methods in the objective clinical assessment of motor function after experimental brachial plexus reconstruction in the rat. J Neurosci Meth 46:203-208.

Bertelli JA, Mira JC (1994) Brachial plexus repair by peripheral nerve grafts directly into the spinal cord in rats. Behavioral and anatomical evidence of functional recovery. J Neurosurg 81:107-114.

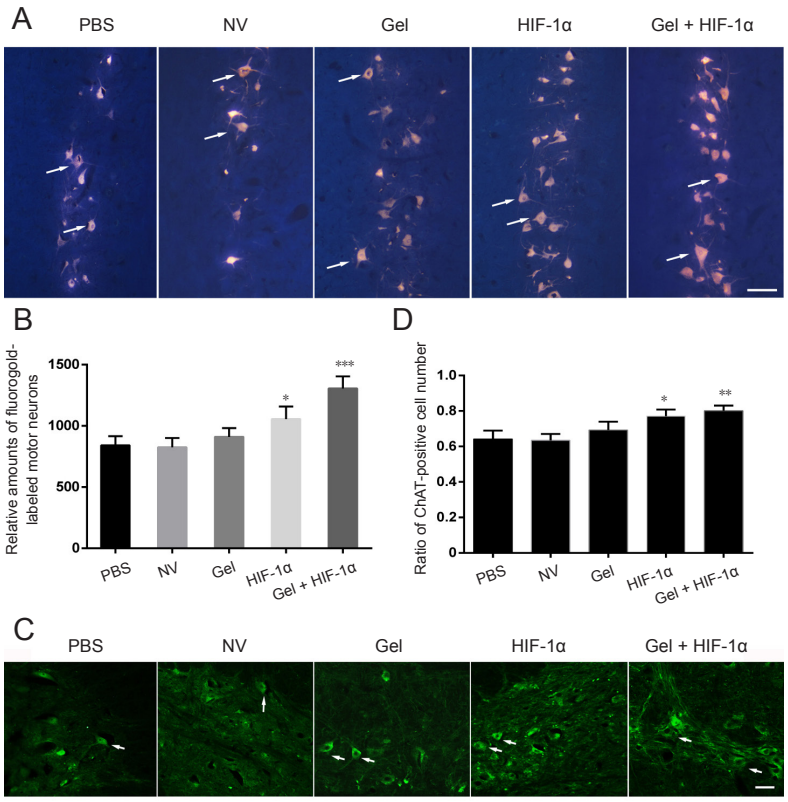

Figure 4 Transplantation of gel + HIF-1α promotes axonal regeneration and reduces neuronal death in ipsilateral spinal segments at 6 weeks after brachial plexus avulsion.

(A) Representative images of fluorogold-labeled motor neurons in ipsilateral C5–7 spinal segments. In total, 2 μL fluorogold was slowly injected into musculocutaneous nerve at the 6-week endpoint and two days before perfusion. Spinal cord segments were collected from each group (n = 4 rats per group). Fluorogold-labeled motor neurons were observed by microscopy of frozen sections. Increased number of fluorogold-labeled cells were observed in the HIF-1α and gel + HIF-1α groups (white arrows: fuorogold-labeled cells; golden yellow: motor neurons). (B) Relative amounts of fluorogold-labeled motor neurons in ipsilateral C5–7 spinal cord at 6 weeks after surgery. (C) Motor neurons in ipsilateral spinal cord (C5–7 segments) were distinguished by immunofluorescence staining with ChAT antibody (cholinergic neuron marker; green: motor neurons) (n = 3 rats per group). Motor neuron loss was visibly decreased by transplantation of gel + HIF-1α. White arrows represent fluorogold-labeled motor neurons. (D) Survival rate of motor neurons was observed by fluorescence microscopy and calculated as a ratio of ChAT-positive cell number in ipsilateral (C5-7 segments) to contralateral spinal cord at 6 weeks after surgery. Data are presented as mean ± SD (one-way analysis of variance followed by the least significant difference *post hoc* test). $*P < 0.05$, $**P < 0.01$, $***P < 0.001$, *vs.* PBS group. Scale bar: 25 μm. FG: Fluorogold; ChAT: choline acetyltransferase; PBS: phosphate buffered saline; NV: negative control of lentivirus; Gel: PF-127 hydrogel; HIF-1α: hypoxia-inducible factor 1α overexpression lentivirus; Gel + HIF-1α: PF-127 hydrogel combined with hypoxia-inducible factor 1α overexpression lentivirus.

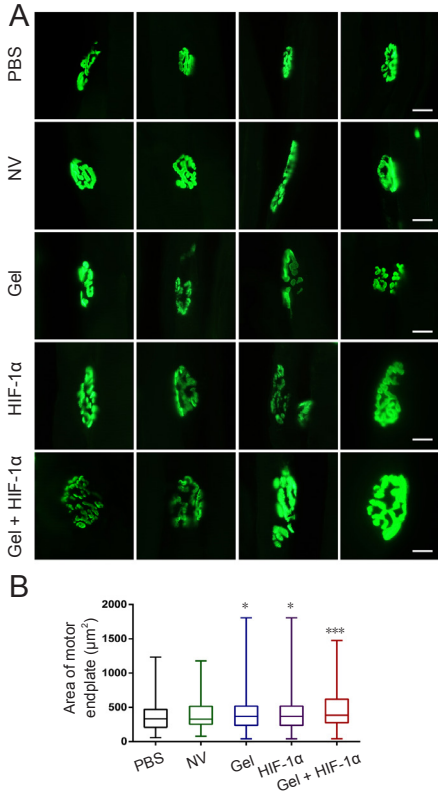

Figure 5 Gel + HIF-1α treatment leads to healthier motor endplates in affected biceps at 6 weeks after brachial plexus avulsion.

(A) Representative images of motor endplates from affected biceps in each treatment group. Immunofluorescence staining for α-BtX (which specifically binds acetylcholine receptors) in affected biceps at 6 weeks post-surgery (green: motor endplates). In rats with reimplantation alone (PBS group) and the NV group, motor endplates were smaller and tended to be faintly stained with an ambiguous appearance. In contrast, motor endplates in the gel, HIF-1α and gel + HIF-1α groups were bigger and had a clear morphology under fluorescence microscope. (B) Average area of motor endplates in all groups at 6 weeks after surgery. Data are presented as the mean ± SD (n = 3; one-way analysis of variance followed by least significant difference *post hoc* test). $*P < 0.05$, $***P < 0.001$, *vs.* PBS group. Scale bar: 100 μm. α-BtX: α-Bungarotoxin; PBS: phosphate buffered saline; NV: negative control of lentivirus; Gel: PF-127 hydrogel; HIF-1α: hypoxia-inducible factor 1α overexpression lentivirus; Gel + HIF-1α: PF-127 hydrogel combined with hypoxia-inducible factor 1α overexpression lentivirus.

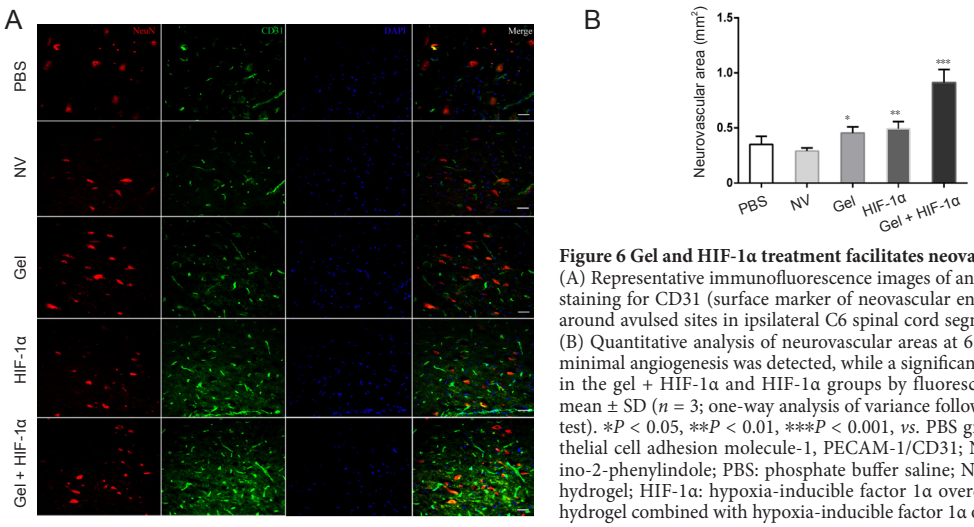

Figure 6 Gel and HIF-1α treatment facilitates neovascularization after brachial plexus avulsion.

(A) Representative immunofluorescence images of angiogenesis and neurons: immunofluorescence staining for CD31 (surface marker of neovascular endothelial cells) and NeuN (neuronal marker) around avulsed sites in ipsilateral C6 spinal cord segments (green: CD31; red: NeuN; blue: DAPI). (B) Quantitative analysis of neurovascular areas at 6 weeks after surgery. In PBS and NV groups, minimal angiogenesis was detected, while a significant increase of neovascularization was observed in the gel + HIF-1α and HIF-1α groups by fluorescence microscopy. Data are presented as the mean ± SD (n = 3; one-way analysis of variance followed by the least significant difference *post hoc* test). $*P < 0.05$, $**P < 0.01$, $***P < 0.001$, *vs.* PBS group. Scale bar: 50 μm. CD31: Platelet endothelial cell adhesion molecule-1, PECAM-1/CD31; NeuN: NEUronal Nuclei; DAPI: 4′,6-diamidino-2-phenylindole; PBS: phosphate buffer saline; NV: negative control of lentivirus; Gel:PF-127 hydrogel; HIF-1α: hypoxia-inducible factor 1α overexpression lentivirus; Gel + HIF-1α: PF-127 hydrogel combined with hypoxia-inducible factor 1α overexpression lentivirus.

Bertelli JA, Taleb M, Mira JC, Calixto JB (1996) Muscle fiber type reorganization and behavioral functional recovery of rat median nerve repair with vascularized or conventional nerve grafts. Restor Neurol Neurosci 10:5-12.

Blits B, Carlstedt TP, Ruitenberg MJ, de Winter F, Hermens WT, Dijkhuizen PA, Claasens JW, Eggers R, van der Sluis R, Tenenbaum L, Boer GJ, Verhaagen J (2004) Rescue and sprouting of motoneurons following ventral root avulsion and reimplantation combined with intraspinal adeno-associated viral vector-mediated expression of glial cell line-derived neurotrophic factor or brain-derived neurotrophic factor. Exp Neurol 189:303-316.

Breidenbach W, Terzis JK (1984) The anatomy of free vascularized nerve grafts. Clin Plast Surg 11:65-71.

Chai H, Wu W, So KF, Yip HK (2000) Survival and regeneration of motoneurons in adult rats by reimplantation of ventral root following spinal root avulsion. Neuroreport 11:1249-1252.

Chai X, Kong W, Liu L, Yu W, Zhang Z, Sun Y (2014) A viral vector expressing hypoxia-inducible factor 1 alpha inhibits hippocampal neuronal apoptosis. Neural Regen Res 9:1145-1153.

Chen HS, Zhou ZH, Li M, Wang JX, Liu BJ, Lu Y (2013) Contribution of brain-derived neurotrophic factor to mechanical hyperalgesia induced by ventral root transection in rats. Neuroreport 24:167-170.

Chin TY, Kiat SS, Faizul HG, Wu W, Abdullah JM (2017) The effects of minocycline on spinal root avulsion injury in rat model. Malays J Med Sci 24:31-39.

Cho Y, Shin JE, Ewan EE, Oh YM, Pita-Thomas W, Cavalli V (2015) Activating injury-responsive genes with hypoxia enhances axon regeneration through neuronal HIF-1alpha. Neuron 88:720-734.

Cibert-Goton V, Phillips JP, Shortland PJ (2015) Vascular changes associated with spinal root avulsion injury. Somatosens Mot Res 32:158-162.

Cullheim S, Carlstedt T, Linda H, Risling M, Ulfhake B (1989) Motoneurons reinnervate skeletal muscle after ventral root implantation into the spinal cord of the cat. J Neurosci 29:725-733.

Diniz IM, Chen C, Xu X, Ansari S, Zadeh HH, Marques MM, Shi S, Moshaverinia A (2015) Pluronic F-127 hydrogel as a promising scaffold for encapsulation of dental-derived mesenchymal stem cells. J Mater Sci-Mater Mater Med 26:153.

Fan X, Heijnen CJ, van der Kooij MA, Groenendaal F, van Bel F (2009) The role and regulation of hypoxia-inducible factor-1alpha expression in brain development and neonatal hypoxic-ischemic brain injury. Brain Res Rev 62:99-108.

Fang XY, Zhang WM, Zhang CF, Wong WM, Li W, Wu W, Lin JH (2016) Lithium accelerates functional motor recovery by improving remyelination of regenerating axons following ventral root avulsion and reimplantation. J Neurosci 329:213-225.

Favier FB, Britto FA, Freyssenet DG, Bigard XA, Benoit H (2015) HIF-1-driven skeletal muscle adaptations to chronic hypoxia: molecular insights into muscle physiology. Cell Mol Life Sci 72:4681-4696.

Feng Y, Liu T, Li XQ, Liu Y, Zhu XY, Jankovic J, Pan TH, Wu YC (2014) Neuroprotection by Orexin-A via HIF-1alpha induction in a cellular model of Parkinson's disease. Neurosci Lett 579:35-40.

Gessi S, Merighi S, Stefanelli A, Fazzi D, Varani K, Borea PA (2013) A(1) and A(3) adenosine receptors inhibit LPS-induced hypoxia-inducible factor-1 accumulation in murine astrocytes. Pharmacol Res 76:157-170.

Gu HY, Chai H, Zhang JY, Yao ZB, Zhou LH, Wong WM, Bruce I, Wu WT (2004) Survival, regeneration and functional recovery of motoneurons in adult rats by reimplantation of ventral root following spinal root avulsion. Eur J Neurosci 19:2123-2131.

Hallin RG, Carlstedt T, Nilsson-Remahl I, Risling M (1999) Spinal cord implantation of avulsed ventral roots in primates; correlation between restored motor function and morphology. Exp Brain Res 124:304-310.

Hao GL, Zhang TY, Zhang Q, Gu MY, Chen C, Zou L, Cao XC, Zhang GC (2018) Partial recovery of limb function following end-to-side screw anastomosis of phrenic nerve in rats with brachial plexus injury. Med Sci Monit 24:4832-4840.

Hao J, Wang X, Bi Y, Teng Y, Wang J, Li F, Li Q, Zhang J, Guo F, Liu J (2014) Fabrication of a composite system combining solid lipid nanoparticles and thermosensitive hydrogel for challenging ophthalmic drug delivery. Colloids Surf B Biointerfaces 114:111-120.

Henderson CE, Phillips HS, Pollock RA, Davies AM, Lemeulle C, Armanini M, Simmons L, Moffet B, Vandlen RA, Simpson LCctSL, Koliatsos VE, Rosenthal A, et al. (1994) GDNF: a potent survival factor for motoneurons present in peripheral nerve and muscle. Science 266:1062-1064.

Hu L, Wang JH, Wang ZL, Xie JY, Chen D, Ding F (2018) Combination of bone morphogenetic protein 2 and mutant hypoxia-inducible factor 1alpha repairs steroid-induced avascular necrosis of the femoral head. Zhongguo Zuzhi Gongcheng Yanjiu 22:4440-4446.

Imanishi M, Tomita S, Ishizawa K, Kihira Y, Ueno M, Izawa-Ishizawa Y, Ikeda Y, Yamano N, Tsuchiya K, Tamaki T (2014) Smooth muscle cell-specific Hif-1alpha deficiency suppresses angiotensin II-induced vascular remodelling in mice. Cardiovasc Res 102:460-468.

Khan M, Khan H, Singh I, Singh AK (2017) Hypoxia inducible factor-1 alpha stabilization for regenerative therapy in traumatic brain injury. Neural Regen Res 12:696-701.

Kizaka-Kondoh S, Inoue M, Harada H, Hiraoka M (2003) Tumor hypoxia: a target for selective cancer therapy. Cancer Sci 94:1021-1028.

Li D, Bai T, Brorson JR (2011) Adaptation to moderate hypoxia protects cortical neurons against ischemia-reperfusion injury and excitotoxicity independently of HIF-1alpha. Exp Neurol 230:302-310.

Li H, Wong C, Li W, Ruven C, He L, Wu X, Lang BT, Silver J, Wu W (2015) Enhanced regeneration and functional recovery after spinal root avulsion by manipulation of the proteoglycan receptor PTPsigma. Sci Rep 5:14923.

Li H, Wu W (2017) Microtubule stabilization promoted axonal regeneration and functional recovery after spinal root avulsion. Eur J Neurosci 46:1650-1662.

Li J, Chen S, Zhao Z, Luo Y, Hou Y, Li H, He L, Zhou L, Wu W (2017) Effect of VEGF on inflammatory regulation, neural survival, and functional improvement in rats following a complete spinal cord transection. Front Cell Neurosci 11:381.

Mills KR (2005) The basics of electromyography. J Neurol Neurosurg Psychiatry 76 Suppl 2:ii32-35.

ELBadawy NE, Abdel-Latif RS, El-Hady HA (2017) Association between SERPINB2 gene expression by real time pcr in respiratory epithelial cells and atopic bronchial asthma severity. Egypt J Immunol 24:165-181.

Oliveira AL, Langone F (2000) GM-1 ganglioside treatment reduces motoneuron death after ventral root avulsion in adult rats. Neurosci Lett 293:131-134.

Pandit NK, McGowan R (1998) Gelation of Pluronic F127-polyethylene glycol mixtures: relationship to PEG molecular weight. Drug Dev Ind Pharm 24:183-186.

Romeo-Guitart D, Fores J, Navarro X (2017) Boosted regeneration and reduced denervated muscle atrophy by NeuroHeal in a pre-clinical model of lumbar root avulsion with delayed reimplantation. Sci Rep 7:12028.

Sato K, Morimoto N, Kurata T, Mimoto T, Miyazaki K, Ikeda Y, Abe K (2012) Impaired response of hypoxic sensor protein HIF-1alpha and its downstream proteins in the spinal motor neurons of ALS model mice. Brain Res 1473:55-62.

Shan T, Ma J, Ma Q, Guo K, Guo J, Li X, Li W, Liu J, Huang C, Wang F, Wu E (2013) β2-AR-HIF-1alpha: a novel regulatory axis for stress-induced pancreatic tumor growth and angiogenesis. Curr Mol Med 13:1023-1034.

Shen YI, Song HG, Papa A, Burke J, Volk SW, Gerecht S (2015) Acellular hydrogels for regenerative burn wound healing: translation from a porcine model. J Invest Dermatol 135:2519-2529.

Su H, Yuan Q, Qin D, Yang X, Wong WM, So KF, Wu W (2013) Ventral root re-implantation is better than peripheral nerve transplantation for motoneuron survival and regeneration after spinal root avulsion injury. BMC Surg 13:21.

Sun Y, Chen X, Zhang X, Shen X, Wang M, Wang X, Liu WC, Liu CF, Liu J, Liu W, Jin X (2017) β2-adrenergic receptor-mediated HIF-1α upregulation mediates blood brain barrier damage in acute cerebral ischemia. Front Mol Neurosci 10:257.

Vleggeert-Lankamp CL (2007) The role of evaluation methods in the assessment of peripheral nerve regeneration through synthetic conduits: a systematic review. J Neurosurg 107:1168-1189.

Wang L, Jiang M, Duan D, Zhao Z, Ge L, Teng X, Liu B, Liu B, Chen P, Lu M (2014) Hyperthermia-conditioned OECs serum-free-conditioned medium induce NSC differentiation into neuron more efficiently by the upregulation of HIF-1 alpha and binding activity. Transplantation 97:1225-1232.

Wang L, Yuzhou L, Yingjie Z, Jie L, Xin Z (2015) A new rat model of neuropathic pain: complete brachial plexus avulsion. Neurosci Lett 589:52-56.

Wu HF, Cen JS, Zhong Q, Chen L, Wang J, Deng DY, Wan Y (2013) The promotion of functional recovery and nerve regeneration after spinal cord injury by lentiviral vectors encoding Lingo-1 shRNA delivered by Pluronic F-127. Biomaterials 34:1686-1700.

P-Reviewer: Tu H; C-Editor: Zhao M; S-Editors: Yu J, Wang J, Li CH; L-Editors: James R, Wysong S, Qiu Y, Song LP; T-Editor: Liu XL